MINERALOGICAL AND OXYGEN ISOTOPIC STUDY OF GROSSITE-BEARING REFRACTORY INCLUSIONS FROM REDUCED CV CHONDRITES.

J. Han[1], K. Nagashima[2], C. Park[3], A. N. Krot[2], and L. P. Keller[4]. [1]Department of Earth and Atmospheric Sciences, University of Houston, Houston TX, 77204, USA (jhan28@central.uh.edu), [2]Hawai'i Institute of Geophysics and Planetology, University of Hawai'i at Mānoa, Honolulu, Hawai'i 96822, USA, [3]Division of Earth-System Sciences, Korea Polar Research Institute, 26 Songdomirae-ro, Yeonsu-gu, Incheon 21990, South Korea, [4]ARES, Code XI3, NASA Johnson Space Center, 2101 NASA Parkway, Houston, TX 77058, USA.

Introduction: Grossite ($CaAl_4O_7$) is predicted to condense as the third major phase, after corundum and hibonite, from a cooling gas of solar composition [1]. Thus, this refractory phase likely preserves a crucial record of high-temperature conditions in the early solar nebula. However, grossite is relatively rare in CAIs from most carbonaceous chondrite groups, except for CH chondrites [2-4]. Only six grossite-bearing CAIs were reported and studied from CV chondrites, and most of them were coarse-grained Type A inclusions [4-6]. Our previous study reported the occurrence of six grossite-bearing, fine-grained Ca-Al-rich inclusions (FGIs) from reduced CV chondrites Efremovka, Thiel Mountains (TIL) 07003, and TIL 07007 [7].

Here we present oxygen isotopic data of grossite-bearing FGIs from reduced CV chondrites to determine if any oxygen isotopic heterogeneity occurs within and among these inclusions. This isotopic study was coordinated with a FIB/TEM study to examine the formation and alteration history of grossite-bearing FGIs in the early solar nebula and on the asteroidal parent body.

Methods: Prior to oxygen isotopic measurements, carbon coating on individual phases of interest was removed by an ion beam using a FEI Quanta 3D FEG dual beam SEM/FIB. Oxygen isotopic compositions of the FGIs were measured in situ with the UH CAMECA ims-1280 SIMS using the method of [e.g., 4].

We reported preliminary TEM results of a grossite-rich nodule on the outer margin of E-B-1 [7]. Additional electron transparent thin sections were extracted from a grossite-rich nodule in three FGIs (TIL 7-05, TIL 7-08, and TIL 7-18) using a FEI Quanta 3D FEG dual beam SEM/FIB. These sections were analyzed using a JEOL 2500SE field-emission STEM to obtain scanning and high-resolution TEM images, electron diffraction patterns, and quantitative EDX data.

Results & Discussion: Similar to grossite-rich nodules in E-B-1 [7], TIL 3-11, TIL 3-16, and TIL 7-18 share a basic nodular structure in which individual nodules have a grossite core surrounded by spinel ± hibonite, melilite, and finally diopside. Perovskite is common in spinel and grossite. Fe-rich phase decorates the boundaries between grossite and spinel and appears extended into grossite. This phase shares a sharp grain boundary with spinel, melilite, and hibonite.

TIL 7-05 consists of spinel-rich nodules, surrounded by melilite, ±anorthite, and diopside. Only the largest nodule contains grossite with Fe-rich veins in the spinel core. In this nodule, abundant perovskite grains are concentrated in the center of the spinel core, and many of them occur adjacent to and within grossite.

TIL 7-08 is mineralogically zoned. The core contains melilite-rich nodules with minor spinel, grossite, perovskite, and hibonite that are separated by a thin layer of diopside. Grossite occurs only in the melilite core, sometimes with perovskite and spinel, but no Fe-rich phase is observed at the SEM scale. The mantle contains spinel-cored nodules with numerous perovskite grains, surrounded by melilite and diopside.
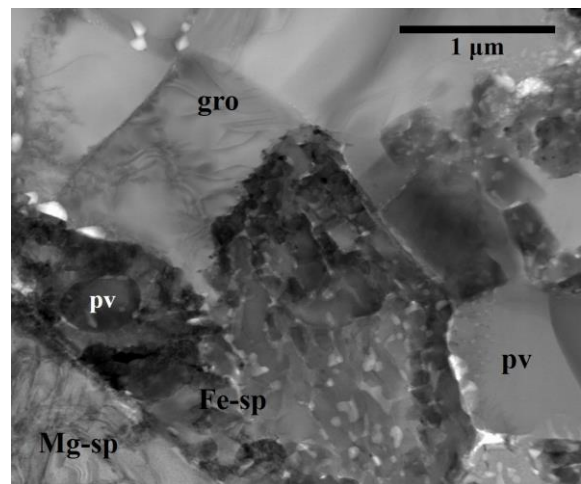
Figure 1. BF STEM image of TIL 7-18, showing grossite and perovskite partially replaced by hercynitic spinel, leaving pores.

TEM results (**Fig. 1**). In three FIB sections from TIL 7-05, TIL 7-08, and TIL 7-18, grossite grains appear to have undergone various degrees of alteration to Fe-rich phase and amorphous material. The Fe-rich phase usually consists of fine-grained aggregates of Zn-bearing (up to 2 wt% ZnO), hercynitic spinel with pores. These aggregates occur as layers separating grossite from Mg-spinel and melilite and as veins between grossite grains. In TIL 7-18, relatively larger, porous hercynitic spinel grains (<5 μm in size) occur with grossite and perovskite. Many pores are interconnected and often faceted with orientation along {111} of the host spinel. All Zn-bearing spinel is a solid solution

(Fe,Mg,Zn)Al_2O_4 and exhibits various atomic ratios of Fe and Mg, with the former usually being higher than the latter. Ca and Mn are also detected in the spinel. In addition, the amorphous material occurs as irregularly-shaped patches and parallel lamellae (<200 nm in thickness) in grossite. The amorphous lamellae are often cross-cutting and oriented normal to the (1-10) and (111) of the host grossite, indicating a degree of crystallographic control. The amorphous material is very Al-rich (>75 wt% Al_2O_3) and contains Ca, Mg, Fe, and Cl.

These observations provide evidence for a preferential alteration of primary grossite in the presence of fluids on the CV chondrite parent body [7,8]. Hercynitic spinel may have directly replaced grossite, with Fe and Zn being supplied from the matrix, while Ca was lost. Mg may have supplied from spinel that experienced minor Fe-Mg interdiffusion and/or from the decomposition of melilite during metamorphism. Alternatively, hercynitic spinel may have precipitated from fluids into an open space formed by the dissolution of primary grossite into amorphous material. The sharp compositional difference between primary Mg-spinel and secondary hercynitic spinel and the survival of numerous pores in hercynitic spinel indicate that the grossite alteration must have occurred after peak metamorphic heating (<500°C; [9]).

Oxygen isotopic compositions (**Fig. 2**). In all FGIs, spinel and hibonite are uniformly ^{16}O-rich ($\Delta^{17}O = -25$ to $-21‰$), whereas perovskite is uniformly ^{16}O-poor ($\Delta^{17}O = -3$ to $-1‰$). Grossite shows nearly uniform ^{16}O-poor compositions ($\Delta^{17}O = -6$ to $-1‰$) within error in all FGIs, except for TIL 7-08 being slightly less ^{16}O-depleted ($\Delta^{17}O = -8$ to $-12‰$).

Melilite exhibits heterogeneous oxygen isotopic compositions between and sometimes within FGIs, with large variations in $\Delta^{17}O$ from -25 to $-2‰$. E-B-1 and TIL 3-11 have a bimodal distribution in which ^{16}O-rich hibonite and spinel occur with ^{16}O-poor melilite and grossite. In TIL 3-16, melilite has intermediate compositions ($\Delta^{17}O = -18$ to $-13‰$) between ^{16}O-rich

spinel and ^{16}O-poor grossite. TIL 7-18 has slightly less ^{16}O-depleted melilite ($\Delta^{17}O = -9‰$) relative to ^{16}O-poor grossite. In TIL 7-05, melilite shows the highest degree of heterogeneous compositions, with $\Delta^{17}O = -23$ to $-2‰$. TIL 7-08 exhibits a progressive ^{16}O depletion from ^{16}O-rich hibonite + spinel, melilite, grossite, finally to ^{16}O-poor perovskite. Only melilite is isotopically heterogeneous in this inclusion, with $\Delta^{17}O = -25$ to $-12‰$.

The observed heterogeneous oxygen isotopic compositions from grossite-bearing FGIs analyzed here are in contrast to uniform ^{16}O-rich compositions of those in CO3.0, CM2, CR3, and CH3.0 chondrites [3,4]. Therefore, we conclude that the oxygen isotopic heterogeneity in grossite-bearing FGIs from reduced CV chondrites are the result of mineralogically-controlled isotope exchange with ^{16}O-poor fluids on the CV chondrite parent asteroid [8,10].

Conclusions: Our FIB/TEM study of grossite-bearing FGIs shows that grossite has been partially altered by metasomatic reaction to hercynitic spinel and amorphous material on cooling after peak metamorphism. Our SIMS measurements of the same inclusions exhibit heterogeneous oxygen isotopic compositions between minerals, indicative of their selective isotopic exchange with ^{16}O-poor fluids. Overall, these provide evidence for a fluid-driven, parent body process during thermal metamorphism.

 References: [1] Grossman L. (2010) MAPS 45, 7-20. [2] Weber D. & Bischoff A. (1994) GCA 58, 3855-3877. [3] Simon S. B. et al. (2019) MAPS 54, 1362-1378. [4] Krot A. N. et al. (2019) Geochemistry 79, 125529. [5] Michel-Lévy M. C. et al. (1982) EPSL 61, 13-22. [6] Maruyama S. and Tomioka N. (2011) MAPS 46, 690-700. [7] Han J. et al. (2022) 85th MetSoc, abstract #6480. [8] Brearley A. J. and Krot A. N. (2013) In: Metasomatism and the Chemical Transformation of Rock, pp. 659-789. [9] Lee M. R. et al. (1996) MAPS 31, 477-483. [10] Krot A. N. et al. (2019) GCA 246, 419-435. [11] McKeegan K. D. et al. (2011) Science 332, 1528-1532.
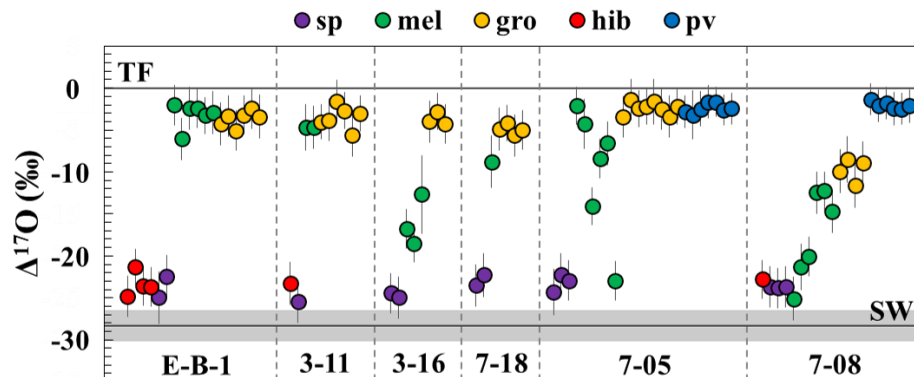
Figure 2. Oxygen isotopic compositions of grossite-bearing FGIs from reduced CV chondrites. SW = Genesis solar wind value ($\Delta^{17}O = -28.4\pm1.8‰$ [11]); TF = terrestrial fractionation line.